Structure of Alanine and Glycine Residues of *Samia cynthia ricini* Silk Fibers Studied with Solid-State ^{15}N and ^{13}C NMR

Tetsuo Asakura,* Takuro Ito, Mami Okudaira, and Tsunenori Kameda

Department of Biotechnology, Tokyo University of Agriculture and Technology, Koganei, Tokyo 184-8588, Japan

Received March 24, 1999; Revised Manuscript Received May 25, 1999

ABSTRACT: The structure of silk fibroin fiber from a wild silkworm, *Samia cynthia ricini*, whose amino acid sequence is similar to the spider (major ampullate) silk, was determined with solid-state NMR. The ^{15}N and ^{13}C labelings for the dominant amino acids, alanine and glycine, residues of *S.c.ricini* silk fibers, were performed by oral administration of [^{15}N]alanine, [1-^{13}C]alanine, [^{15}N]glycine, or [1-^{13}C]glycine to the fifth instar larvae of the silkworm, *S.c.ricini*. The blocks of the oriented silk fibers, stretched by about 10 times the original length of the sample, were prepared, and the ^{15}N and ^{13}C solid-state NMR were observed by changing the angles of the oriented silk fiber axis and the magnetic field. All of the oriented spectra of [^{15}N]glycine silk fibroin fiber and [1-^{13}C]glycine silk fibroin fiber were slightly broader than the corresponding spectra of alanine isotope-labeled silk fibers. The fraction of alanine residues in oriented domains in the silk fiber samples was 75%, and that of glycine residues was 65%. The specific orientations of NH, NC′, C′O, and C′N bonds for alanine and glycine residues in the oriented domain were determined from the angle-dependent spectra. The conformational space for the alanine and glycine residues was substantially reduced with these bond orientations, and the best fit torsion angles, ϕ and ψ, within the reduced conformational space were determined. The torsion angles of these two residues were within antiparallel β-sheet structural region.

Introduction

The silk fibroins from silkworms can produce strong, stiff fibers at room temperature and from an aqueous solution, whereas synthetic materials with comparable properties must be processed at higher temperatures and/or from less benign solvents. The properties of natural silk fiber are the consequence not only of the chemical composition but also of the conditions under which the bulk silk secretions are converted into fiber—they depend on the molecular order in the fiber. Thus, it is important to study molecular structure of the silk including the molecular alignment in order to clarify the origin of the impressive mechanical properties.[1]

The silk fibroin from the domesticated silkworm, *Bombyx mori*, is a well-known fibrous protein whose amino acid composition (in mole percent) is 42.9% glycine, 30.0% alanine, 12.2% serine, 4.8% tyrosine, and 2.5% valine.[2] The detailed primary structure has recently been reported by Mita et al.[3] The secondary structure of the silk fibroin fiber was proposed by Marsh et al.[4] to be antiparallel β-sheet, on the basis of X-ray diffraction studies and by assuming that the sequence was -(Gly-Ala)$_n$-. This structural model has been supported by more detailed X-ray diffraction analyses[5,6] and IR studies[7] as well as conformation-dependent ^{13}C and ^{15}N solid-state NMR chemical shifts.[8−13]

In contrast, the amino acid composition of silk fibroin from a wild silkworm, *Samia cynthia ricini*, is different from that of *B.mori* silk fibroin. The sum of Gly and Ala residues is 82%, which is basically the same as that of *B.mori* silk (71%), but the relative composition of Ala and Gly is reversed.[2] The proportion of Gly residues is greater in *B.mori* silk fibroin, while the content of Ala residues is greater in *S.c.ricini* silk fibroin. The primary structure of the silk fibroin from *S.c.ricini* has recently been determined by Yukihiro et al.,[14] which was very similar to the structure of silk fibroin from *Antheraea pernyi*.[15] Namely, the silk mainly consists of the repeated similar sequences by about 100 times where there are alternative appearances of polyalanine region and glycine-rich region like spider (major ampullate) silk. From the solution ^{13}C and ^{15}N NMR studies of *S.c.ricini* silk fibroin in aqueous solution, it is evaluated that about 70% of Ala residues form α-helices, while the conformation of the other Ala residues is random coil.[16−18] The solution structure of most of the other residues including Gly residue seems to be random coil because there was no significant chemical shift changes indicative of a helix−coil transition, with increasing temperature, although 70% of the Ala residues exhibited a chemical shift change due to fast exchange between the two conformations.[16,17] The antiparallel β-sheet structure has also been proposed for the Ala residues of *S.c.ricini* silk fiber in the solid state on the basis of the conformation-dependent ^{13}C chemical shift.[8] However, there is no structural information for the Gly residues of *S.c.ricini* silk fiber because of the small conformation-dependent chemical shift.[12,13,19]

In general, the primary contributing method for high-resolution determination of structure has been X-ray diffraction from single crystals, which has provided detailed blueprints of the molecular architecture of numerous proteins. However, the application of X-ray crystallography has been restricted to proteins from which well-ordered crystals can be grown. This difficulty has excluded a large number of biologically relevant proteins and has been the impetus for the development of new techniques for determining atomic resolution structures. Fibrous proteins are particularly difficult to study using standard structure determination techniques. The X-ray diffraction from fibers in which proteins are aligned along the long axis of the fiber typically yields general features of molecular organization and packing but lacks atomic resolution details.

10.1021/ma990442z CCC: $18.00
Published on Web 07/07/1999

High-resolution solution NMR techniques are not applicable to fibrous proteins, since the solution-state structure is generally not representative of the structure in the fibrous state. However, the natural alignment of the protein within the fiber provides an important advantage that can be analyzed by solid-state NMR.[20−22]

The solid-state ^{15}N NMR spectra of *B.mori* silk fiber obtained from uniaxially aligned molecules placed with the axis of alignment both parallel and perpendicular to the magnetic field were reported and analyzed to yield the orientations of specific molecular bonds. The NMR-derived and the fiber diffraction-derived angles between the NH and NC′ bond vectors and the fiber axis agree well for the [^{15}N]Gly site.[20] Most recently, the torsion angles, ϕ and ψ, of Ala and Gly residues of *B.mori* silk fibroin fiber were determined from ^{15}N and^{13}C solid-state NMR spectroscopies.[22] For this purpose, [^{15}N]Ala, [^{15}N]Gly, [1-^{13}C]Ala, and [1-^{13}C]Gly sites of the silk fibroin were highly labeled by oral administration of the isotope-labeled amino acids to fifth silkworm larvae or by cultivation of the silk glands in a medium containing the isotope-labeled amino acids.[23] The specific NH and NC′ bond orientations relative to the fiber axis were determined for both Ala and Gly residues from the^{15}N solid-state NMR spectra of the uniaxially aligned ^{15}N-labeled silk fibroin fibers.[20] Similarly, the C′O and C′N bond orientations were determined for both Ala and Gly residues from the ^{13}C solid-state NMR spectra of ^{13}C-labeled silk fibers.[24] Subsequently, the torsion angles, ϕ and ψ, were calculated by combining these bond orientations for both Ala and Gly residues.

In this paper, the solid-state NMR analyses developed for the structural determination of *B.mori* silk fibers were applied to determine the torsion angles, ϕ and ψ, of Ala and Gly residues in the oriented domain of *S.c.ricini* silk fibroin fiber. The ^{15}N and ^{13}C labelings of the *S.c.ricini* silk fiber were performed for the Ala and Gly residues by oral administration of isotope-labeled amino acids. The fraction of oriented and nonoriented domains in the silk samples was determined from the ^{15}N and ^{13}C solid-state NMR spectra of the blocks of the oriented silk fibers observed by changing the angles of the oriented silk fiber axis and the magnetic field. Because of the small conformation-dependent isotropic chemical shift[12,13,19] for the Gly residue, the solid-state NMR analysis which is characteristic of the oriented structure used here is especially useful for the structure determination of the Gly residues of *S.c.ricini* silk fiber where large amounts of Gly residue are present in a variety of the Gly-containing sequences in the chain. In addition, the structure of the Gly residues in spider silk will be also discussed by reference to the structure of the Gly residues in *S.c.ricini* silk fibroin determined here because of the similar primary structures with each other.

Materials and Methods

^{15}N and ^{13}C Labelings of Silk Fibroin. From eggs of *S.c.ricini* (which were kindly supplied by Dr. Jun Saito, National Institute of Sericultural and Entomological Science, Tsukuba, Japan), larvae were reared on *Ailanthus glandulosa* leaves in our laboratory.[16,25,26] A 100 μL aliquot of 10% (w/v) [^{15}N]alanine (99.9 at. % ^{15}N enrichment, Mastrace, Inc., Woburn, MA) in aqueous solution was given by oral administration to fifth instar larvae from 3-day-old to 6-day-old for 4 days: two times, morning and evening, per day for a silkworm. Then the 7-day-old fifth instar larva was anesthetized in ice-cold water for 10 min and sterilized by immersing in 70% ethanol solution. The silk gland consisting of the anterior, middle, and posterior divisions was pulled out with forceps from a small incision on the abdominal side of the head−thorax intersegment. The silk glands containing [^{15}N]-Ala silk fibroins were then washed twice in ice-cold 1.15% potassium chloride solution. Similarly, [^{15}N]glycine (99.9 at. % ^{15}N enrichment, Mastrace, Inc., Woburn, MA), [1-^{13}C]alanine (99.9 at. % ^{13}C enrichment, Mastrace, Inc., Woburn, MA), and [1-^{13}C]glycine (99.9 at. % ^{13}C enrichment, Mastrace, Inc., Woburn, MA) were used to obtain [^{15}N]Gly, [1-^{13}C]Ala, and [1-^{13}C]Gly silk fibroins, respectively.

Preparation of Oriented Block Samples. The silk glands containing silk fibroins were immersed in the dilute acetic acid (1%) for 15 min. The glands were washed carefully by gently agitating the acid solution to remove contaminants, and the structure of the silk at the surface was changed to β-sheet structure. Then the silk glands containing silk fibroins were stretched by about 10 times the original length of the sample under constant speed with a motor and wound onto a glass tube. During the process, the lining of the silk glands was easily removed by gently applying pressure to the surface of the silk gland. To prepare blocks of oriented fibers, the silk fibers were placed on a treating apparatus with handle, which produces sheets of highly oriented fibers. These sheets were fixed in place with quick-setting epoxy and then cut into 6 mm $\times$ 10 mm pieces, stacked together, and fixed with epoxy to form an 6 mm $\times$ 10 mm $\times$ 4 mm block that fit within the radio-frequency coil of the NMR probe. This winding procedure ensures essentially uniform alignment of the macroscopic fiber axis; any further misalignment can be attributed to local orientational distributions of the polypeptide backbone relative to the macroscopic fiber axis. Four kinds of silk fibroin fiber blocks—[^{15}N]Ala, [^{15}N]Gly, [1-^{13}C]Ala, and [1-^{13}C]Gly silk fibroins—were prepared for NMR observation.

NMR Observation. The static and magic-angle spinning (MAS) solid-state ^{15}N NMR and ^{13}C experiments were performed at 25° C with a CMX Infinity 400 NMR spectrometer (Chemagnetics) operating at 40.3 and 100.0 MHz, respectively. Cross-polarization was employed for sensitivity enhancement with high-power ^{1}H decoupling during the signal acquisition period. Typical NMR parameters were as follows: 7 μs 90° pulse with a 1 ms mixing time, 5 s repetition delay, and 10 000 scans for ^{15}N NMR, and 5.9 μs 90° pulse with a 1 ms mixing time, 5s repetition delay, and 10 000 scans for ^{13}C NMR. Phase cycling was used to minimize artifacts. The orientation-dependent ^{15}N and ^{13}C solid-state NMR spectra were observed when the fiber axis was arranged at various angles between 0° and 90° to the magnetic field direction. The ^{15}N chemical shifts were referenced to $^{15}NH_4NO_3$ by setting the signal of solid $^{15}NH_4Cl$ to 18.0 ppm, and ^{13}C chemical shifts were referenced to $(CH_3)_4Si$ by setting the signal of solid adamantane to 29.5 and 38.6 ppm. The chemical shift tensor components were determined from the slow MAS sideband intensities by the Herzfeld and Berger method.[27]

Simulations of Solid-State NMR Spectra. The orientation-dependent ^{15}N and ^{13}C solid-state NMR spectra were simulated on the basis of the chemical shift anisotropy to determine the Euler angles, α_F and β_F, that relate the principal axis system (PAS) to the fiber axis coordinate system. A trial-and-error process was utilized to simulate the solid-state NMR spectra by varying α_F and β_F. A Gaussian probability distribution of fiber axis orientations, p, was employed to account for the spectral broadening. The Euler angles, α_D and β_D, for transforming the PAS to molecular symmetry axis (MSA) system, determined from the simulation of ^{13}C−^{15}N dipolar modulated powder pattern of the [1-^{13}C]−[^{15}N] doubly labeled model peptides[28,29] were also used. The specific orientations of NH, NC′, C′O, and C′N bonds for Ala and Gly residues in the oriented domain of the silk fibroin fiber were determined with a combination of these Euler angles. The conformational space for the Ala and Gly residues of the silk fibroin fiber was substantially reduced with these bond orientations, and the best fit torsion angles, ϕ and ψ, within the reduced conformational space were determined. Details of the simulation

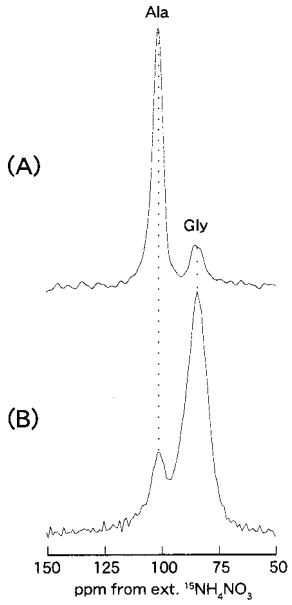

Figure 1. Solid-state ^{15}N CP/MAS NMR spectra of (A) [^{15}N]-Ala and (B) [^{15}N]Gly labeled *S.c.ricini* silk fibroin fibers.

Table 1. ^{13}C and ^{15}N Chemical Shift Tensors and Isotropic Chemical Shifts for Gly and Ala Residues

	[^{15}N]Ala[a]	[^{15}N]Gly[a]	[1-^{13}C]Ala[b]	[1-^{13}C]Gly[b]
σ_{11}	34.2	21.0	85.5	89.2
σ_{22}	67.6	53.0	190.3	178.0
σ_{33}	200.8	182.1	241.4	241.5
σ_{iso}	101.0	84.6	172.4	169.5

[a] Parts per million (ppm) from external $^{15}NH_4NO_3$. [b] Parts per million (ppm) from external TMS.

including the definition of these Euler angles are described eleswhere.[22] All of the calculations were performed with a Mips Fortran 77 compiler on a Unix workstation (Silicon Graphics, Inc., Indy R4400, IRIX5.3).

Results

Isotropic ^{15}N and ^{13}C Chemical Shifts. Figure 1 shows ^{15}N CP/MAS NMR spectra of [^{15}N]Ala and [^{15}N]-Gly silk fibroin fibers stretched by about 10 times the original silk fiber. The isotropic chemical shift σ_{iso} value of the [^{15}N]Ala residues is larger than the value of [^{15}N]-Gly residues by 15.4 ppm (Table 1),[12] which is in agreement with the previous chemical shift data. It is clear that the isotopic enrichments of [^{15}N]Ala and [^{15}N]-Gly labeled samples are high enough for ^{15}N NMR analyses of each site. The isotropic chemical shift σ_{iso} value of the [^{15}N]Ala residues,101 ppm, indicates that Ala sequences in the chain take β-sheet structure.[12] On the other hand, a broader peak than the Ala peak by about 2 times indicates there are several kinds of structures reflecting the chemical shift distribution for the Gly sites.[18] Actually, four peaks split into several sequences are observed in the Gly peak region of the ^{15}N solution spectrum of *S.c.ricini* silk fibroin. The ^{13}C CP/MAS NMR spectra of [1-^{13}C]Ala and [1-^{13}C]Gly silk fibroin fibers (10 times stretching ratio) are shown in Figure 2. The chemical shift, 20 ppm, of the Ala C_β peaks in both samples indicates the Ala sequences take the β-sheet structure, which was the same as the results from ^{15}N NMR mentioned above.[12] The carbonyl carbon chemical shifts of Ala residues are also in agreement with the β-sheet structure. These data indicate that the structure is basically the same between the silk fiber prepared by stretching the silk stored in a silk gland by a factor of 10 and the spun silk obtained from a cocoon.

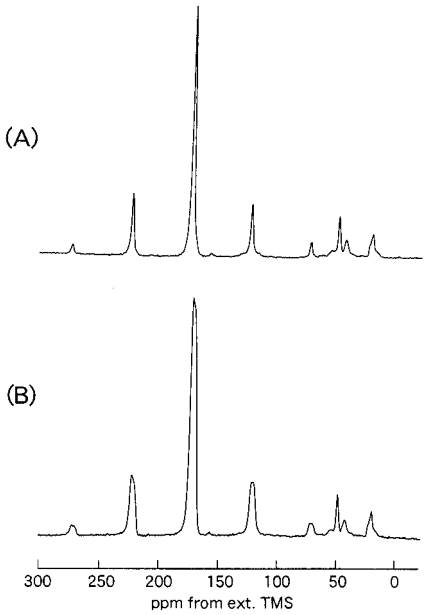

Figure 2. Solid-state ^{13}C CP/MAS NMR spectra of (A) [1-^{13}C]-Ala and (B) [1-^{13}C]Gly labeled *S.c.ricini* silk fibroin fibers.

Chemical Shift Tensors. In analyzing the local structure of Ala and Gly sites, it is necessary to determine the chemical shift tensors of ^{15}N and carbonyl ^{13}C nuclei for both Ala and Gly sites. With spinning sideband analysis developed by Herzfeld and Berger,[27] the chemical shift tensor values were determined: The ^{15}N CP/MAS NMR spectra of [^{15}N]Ala and [^{15}N]Gly silk fibroin fibers were observed and simulated by changing the spinning rates from 1400 to 1800 Hz. The similar observations and simulations were performed for [1-^{13}C]-Ala and [1-^{13}C]Gly silk fibroin fibers. The chemical shift tensors determined are listed in Table 1. The σ_{iso} value calculated from three chemical shift tensors is in agreement with σ_{iso} value determined with CP/MAS NMR. These data can be used for further structure analysis of *S.c.ricini* silk fibroin fibers.

^{15}N CP NMR Spectra of Oriented Samples. Figure 3 shows the ^{15}N solid-state NMR spectra of [^{15}N]Ala and [^{15}N]Gly silk fibroin fiber blocks aligned with the fiber axis, which are set as a function of the angle between the fiber axis and magnetic field B_0 together with the powder pattern spectra. The ^{15}N spectra of silk blocks change largely by changing the angles, indicating that both samples are oriented significantly. This observation is the same as those for [^{15}N]Ala and [^{15}N]Gly *B.mori* silk fibroin fibers reported previously although the sequence of *S.c.ricini*. silk fibroin is quite different from *B.mori* silk fibroin. Namely, for *B.mori* silk fibroin, Ala and Gly residues are mainly present in the alternative sequences such as ...-Ala-Gly-Ala-Gly-Ala-Gly-.[3] However, *S.c.ricini* silk fibroin mainly consists of the repeated similar sequences by about 100 times where there are alternative appearances of polyalanine region and glycine-rich region like spider (major ampullate) silk.[14,30−33] For the Ala sequence, it is well-known that there is a strong tendency to form an α-helix which was predicted using the Chou−Fasman scheme[34] for predicting secondary structure. Actually, in the aqueous solution of the silk fibroin, the sequence takes an α-helix as reported previously from the solution NMR of the silk fibroin stored in the silk gland of *S.c.ricini* silkworm.

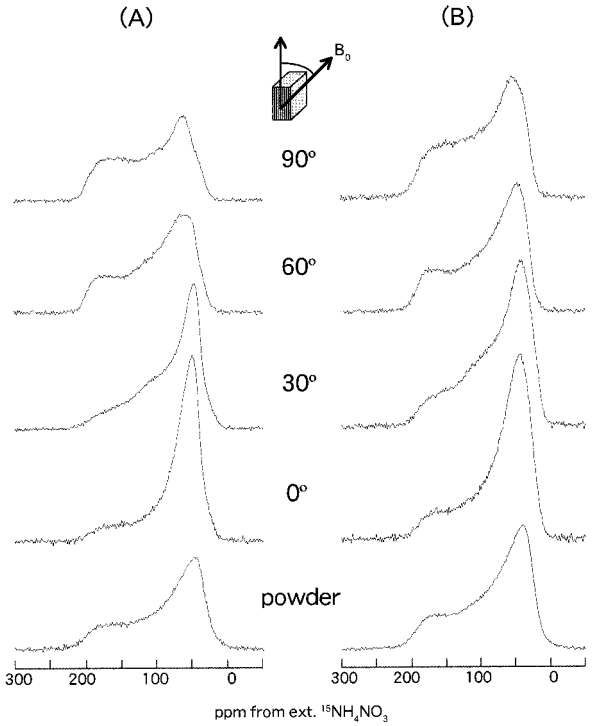

Figure 3. Solid-state ^{15}N CP NMR spectra of an oriented block of (A) [^{15}N]Ala and (B) [^{15}N]Gly *S.c.ricini* silk fibroin fibers as a function of the angle between the fiber axis and the magnetic field B_0.

However, the silk fibroin is converted into the β-sheet structure which is stabilized by the formation of intermolecular hydrogen bonding by stretching the silk by 10 times its original length. This seems reasonable because the β-sheet structure can be formed for even shorter sequence of Ala sequence in spider silk[30−33] (5−7 Ala residues in spidroin 1 and 6−10 residues in spidroin 2, while 11−14 Ala residues in *S.c.ricini* silk fibroin).

It is especially interesting to discuss the orientation and conformation of Gly residues in *S.c.ricini* silk fibroin fiber with the angle-dependent analytical method used here because the ^{13}C and ^{15}N chemical shifts of Gly residue are generally insensitive to the conformation of the Gly residue. Figure 3B shows clearly there is oriented Gly residue at the Gly-rich region by stretching 10 times. This spectral behavior is similar to that of the Ala residue taking the β-sheet structure. However, all of the oriented spectra of [^{15}N]Gly silk fibroin fiber blocks are slightly broader than the spectra of [^{15}N]Ala silk fibroin fiber blocks, and the fraction of oriented components is smaller than the latter case.

Figure 4 is a series of spectra of oriented components of [^{15}N]Gly silk fibroin fiber blocks obtained by subtraction of the powder pattern component from the oriented spectra along with the simulated spectra for determination of the Euler angles, α_F and β_F. Here, the angles α_F and β_F are defined as angles which relate the principal axis system to the fiber axis coordinate system. The detailed definition and interpretation of these Eular angles were described previously.[20,22] The α_F and β_F values determined are listed in Table 2 along with the value, p, which indicate the distribution of the fiber axis obtained by assuming a Gaussian distribution. A similar spectral analysis was performed for [^{15}N]Ala silk fibroin fiber blocks, and the results are also listed in Table 2. The fraction of oriented components is 75% for the Ala site and 65% for the Gly site. The p values are larger

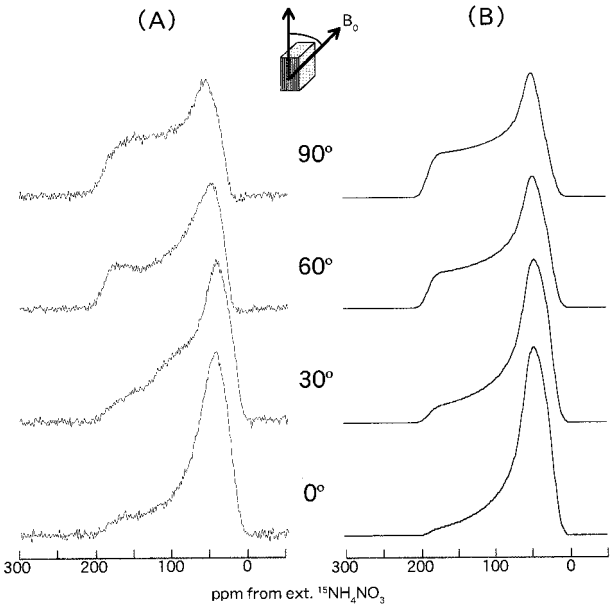

Figure 4. Solid-state ^{15}N CP NMR spectra of an oriented block of [^{15}N]Ala *S.c.ricini* silk fibroin fibers(A) as a function of the angle between the fiber axis and the magnetic field B_0. Noncrystalline fraction in the silk fibroin fibers has been determined by subtracting the powder pattern from these spectra. The simulated spectra are shown in (B). The distribution of the fiber axis orientation, p, was determined to be 23°. The Euler angles determined are listed in Table 2.

Table 2. Euler Angles, α_F, β_F, and Distribution of Fiber Axis, p, for [^{15}N]Ala, [^{15}N]Gly, [1-^{13}C]Ala, and [1-^{13}C]Gly Sites in *S.c.ricini* Silk Fibroin Fiber

	[^{15}N]Ala	[^{15}N]Gly	[1-^{13}C]Ala	[1-^{13}C]Gly
p (deg)	23	31	23	31
α_F (deg)	25	25	80	80
β_F (deg)	73	70	160	165
oriented component (%)	75	65	75	65

The fraction of Oriented Component is also listed.

for [^{15}N]Gly silk fibroin fiber than [^{15}N]Ala silk fibroin fiber. The α_F and β_F values are almost the same between the two ^{15}N sites and are almost the same as those for *B.mori* silk fibroin fiber.

[1-^{13}C] CP NMR Spectra of Oriented Samples. The ^{13}C CP spectra can be obtained within shorter accumulation times than the ^{15}N CP spectra because of the higher sensitivity of ^{13}C nuclei. However, the peaks from the bonding reagents for preparation of the silk fiber blocks are also observed together with the natural abundance spectra of the silk fibroin fibers. Thus, the ^{13}C spectra shown in Figure 5 are obtained by subtracting the spectra of oriented natural abundance silk fibroin fibers containing the bonding reagents from the original spectra of [1-^{13}C]Ala and [1-^{13}C]Gly silk fibroin fiber blocks. Similar to the ^{15}N NMR spectra in Figure 3, the ^{13}C spectra of oriented silk blocks change significantly by changing the angles between the fiber axis and magnetic field B_0. This also indicates that both samples are well-oriented although the appearance of the peak at around 180 ppm in the oriented [1-^{13}C]Gly silk fibroin fiber blocks at the angles of 0° and 30° indicates that there are relatively larger amounts of powder pattern components in the Gly sites in the oriented samples compared with the oriented [1-^{13}C]Gly silk fibroin fiber blocks.

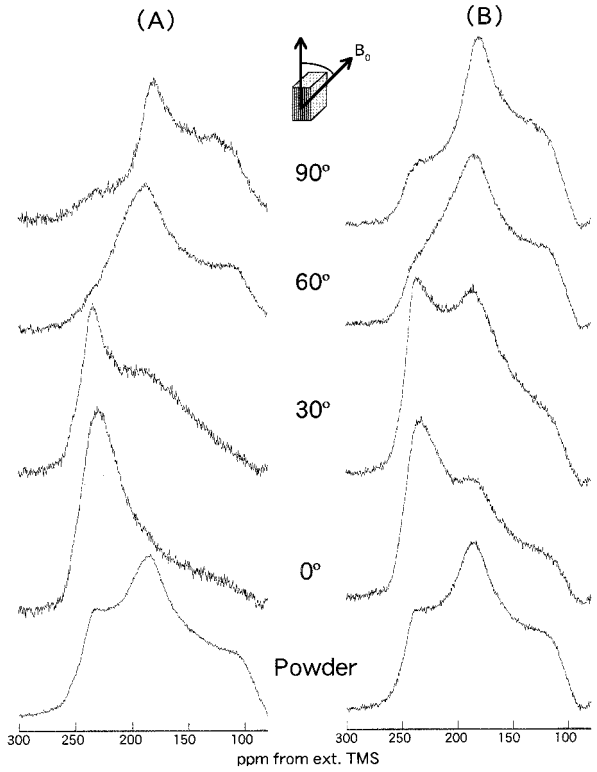

Figure 5. Solid-state ^{13}C CP NMR spectra of an oriented block of (A) [1-^{13}C]Ala and (B) [1-^{13}C]Gly *S.c.ricini* silk fibroin fibers as a function of the angle between the fiber axis and the magnetic field B_0.

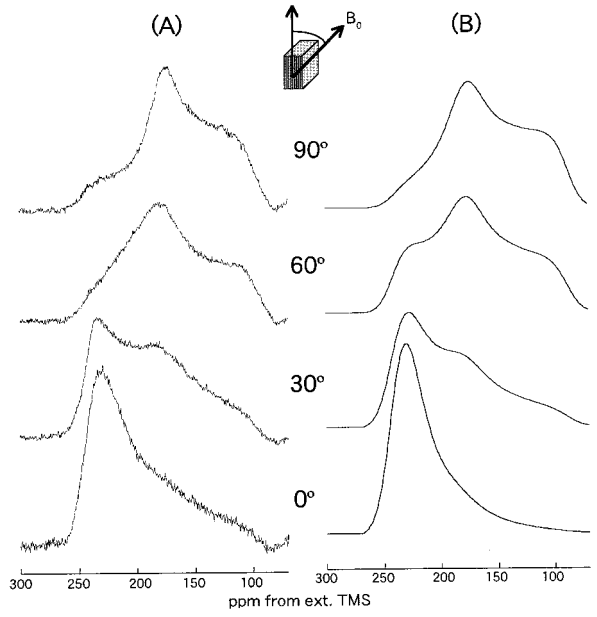

Figure 6. Solid-state ^{13}C CP NMR spectra of an oriented block of [1-^{13}C]Gly *S.c.ricini* silk fibroin fibers (A) as a function of the angle between the fiber axis and the magnetic field B_0. Noncrystalline fraction in the silk fibroin fibers has been determined by subtracting the powder pattern from these spectra. The simulated spectra are shown in (B). The distribution of fiber axis orientation, *p*, was determined to be 31°. The Euler angles determined are listed in Table 2.

Figure 6 is a series of spectra of only the oriented components of [^{15}N]Gly silk fibroin fiber blocks obtained by subtraction of the powder pattern components from the original oriented spectra in Figure 5 along with the simulated spectra for determination of the Euler angles, α_F and β_F. The fraction of the powder components was also determined to be 35%, which is the same value determined from oriented [^{15}N]Gly silk fibroin fiber blocks in Figure 3. Similar simulation was also performed for [1-^{13}C]Ala silk fibroin fiber blocks. The α_F, β_F, and *p* values for both sites are summarized in Table 2. The fraction of powder pattern components decreased to 25%, which is in agreement with the ^{15}N Ala data. The *p* value for [1-^{13}C]Ala silk fibroin fiber block is 23 and also became smaller than the value, 31, for [1-^{13}C]-Gly silk fibroin fiber block. The *p* value reported for oriented *B.mori* silk fibroin fibers was 10, and therefore the distribution of the fiber axis is larger for *S.c.ricini* silk fiber than for *B.mori* silk fiber even in the Ala sites.

Determinations of ϕ and ψ Angles of Ala and Gly Residues in the Oriented Domain. The α_F and β_F values determined for the Ala and Gly residues in the oriented components can be used for determination of the torsion angles, ϕ and ψ, by the combination of the Euler angles of the ^{13}C and ^{15}N CSA PAS system, relative to the MSA system for [1-^{13}C]Ala, [1-^{13}C]Gly, [^{15}N]Ala, and [^{15}N]Gly sites. These Euler angles for each site were already reported with the model compounds for *B.mori* silk fibroins, Boc-Gly-Ala-[1-^{13}C]Gly-[^{15}N]Ala-Gly-Ala-OPac and Boc-Ala-Gly-[1-^{13}C]Ala-[^{15}N]Gly-Ala-Gly-OPac.[29] For example, the ^{13}C powder pattern spectrum of [1-^{13}C]Gly is modified by the dipolar interaction with [^{15}N]Ala. The same dipolar interaction is also observed in the^{15}N powder pattern spectrum. The Euler angles of the ^{15}N CSA PAS relative to the MSA system for the [1-^{13}C]Gly-[^{15}N]Ala doubly labeled model peptide can be determined from the simulation of the $^{13}C-^{15}N$ dipolar modulated powder pattern using the approach described by Teng and Cross. Using the simulation for the ^{15}N powder pattern spectrum including the dipolar interaction, the Euler angles of the ^{15}N CSA PAS relative to the MSA system, α_{DNC} and β_{DNC}, were determined as $\alpha_{DNC} = 0 \pm 5°$ and $\beta_{DNC} = 109 \pm 2°$ for the ^{15}N Ala site. These angles indicate that there is the σ_{33} component of ^{15}N nuclei in the C−N−H plane. On the other hand, the Euler angles of the ^{13}C CSA PAS relative to the MSA system for the [1-^{13}C]Gly-[^{15}N]Ala doubly labeled model peptide, α_{DCN} and β_{DCN}, for the Gly site were determined as $\alpha_{DCN} = 0 \pm 5°$ and $\beta_{DCN} = 35 \pm 2°$ from the simulation of the ^{13}C powder pattern spectrum.[29] These Euler angles indicate that there is the σ_{22} component of ^{13}C nuclei in the N−C−O plane.[29] Similarly, the Euler angles of the ^{15}N Gly site were determined as $\alpha_{DNC} = 0 \pm 5°$, and those for the ^{13}C Ala site, $\alpha_{DCN} = 0 \pm 5°$ and $\beta_{DCN} = 33 \pm 2°$. Then the bond orientations with respect to the fiber axis, θ_{NH}, θ_{NC} for ^{15}N Gly and ^{15}N Ala sites and θ_{CO}, θ_{CN} for [1-^{13}C]Gly and [1-^{13}C]Ala sites, are calculated by the combination of these Euler angles as reported previously.[22] The angles are $\theta_{NH} = 86°$, $\theta_{NC} = 42°$ for the [^{15}N]Gly site and $\theta_{NH} = 85°$, $\theta_{NC} = 44°$ for the [^{15}N]Ala site. Similarly, $\theta_{CO} = 88°$, $\theta_{CN} = 140°$ for the [1-^{13}C]Gly site and $\theta_{CO} = 86°$, $\theta_{CN} = 139°$ for [1-^{13}C]Ala. By taking into account the experimental error, the $\phi-\psi$ constraints for Ala and Gly residues are determined as shown in Figure 7. These results suggest that the $\phi-\psi$ constraints are able to be reduced. The final $\phi-\psi$ values are summarized in Table 3.

Discussion

The $\phi-\psi$ angles of Ala and Gly residues in the oriented domain of *S.c.ricini* silk fibers were determined. These angles were almost the same as those

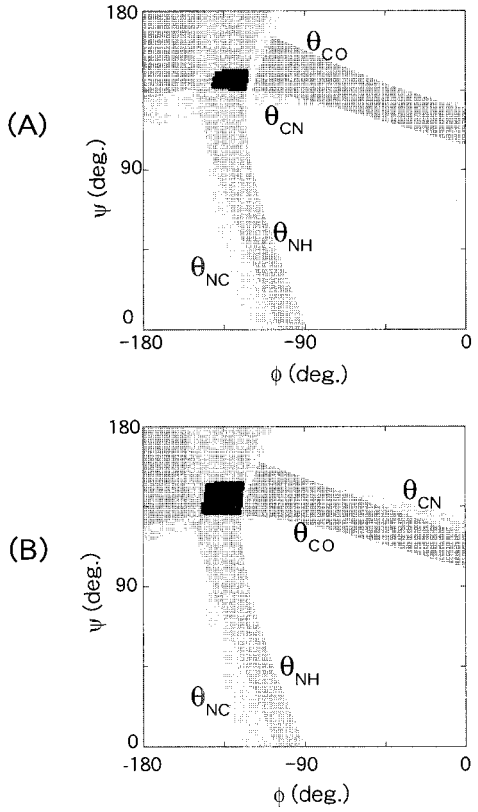

Figure 7. Variation in bond orientations, θ_{NH}, θ_{NC}, θ_{CO}, and θ_{CN}, as a function of torsion angles (ϕ, ψ) constrained by the $C_{\alpha(i-1)}-C_{\alpha(i+1)}$ axis being parallel to the FAS and by NMR orientational constraints for (A) Ala and (B) Gly residues. The conformational space is restricted to an experimental error of ±5° for each bond orientation.

Table 3. Torsion Angles (ϕ, ψ) of *S.c.ricini* Silk Fibroin Fibers Determined from Solid-State NMR

	ϕ (deg)	ψ (deg)
Ala	−142 to −122	135−146
Gly	−140 to −125	131−148

obtained for *B.mori* silk fibroins. It is easily predicted that the Ala sequences in the *S.c.ricini* silk fibers take the β-sheet structure from the ^{15}N isotropic chemical shift σ_{iso} value of the [^{15}N]Ala nitrogen and ^{13}C isotropic chemical shifts of Cα, Cβ and carbonyl carbons in the CP/MAS NMR spectra. However, from the more detailed structural analysis used here, the $\phi-\psi$ constraints were obtained in the β-sheet region of the Ramachandran map. These angles are for the Ala residues in the oriented regions, which is 75% of the total Ala residues. The other Ala residues give powder pattern spectra, indicating that these are in a nonoriented region.

Since the ^{13}C and ^{15}N chemical shifts of Gly residue are generally insensitive to the conformation of the Gly residue, the solid-state NMR analysis which is characteristic of the oriented structure used here is especially useful for the structure determination of the Gly residues of *S.c.ricini* silk fiber. The conformation of most of the Gly residues in *S.c.ricini* silk fibroin in aqueous solution which is stored in the silk gland is random coil. This conclusion was derived from our solution NMR study: The Gly carbonyl carbon peak, which was split into 10 peaks depending on the different Gly environments in the sequences of the chain, did not change through the helix−coil transition of the Ala sequences.[16,17,35]

In the solid state, the Gly-rich region of the *S.c.ricini*. silk fibroin fiber stretched by 10 times takes the β-sheet structure as well as the Ala sequences, which was derived from a detailed analysis of the oriented NMR data as mentioned above. This observation is the same as those for [^{15}N]Ala and [^{15}N]Gly *B.mori* silk fibroin fibers reported previously although the sequence of *S.c.ricini*. silk fibroin is quite different from *B.mori* silk fibroin. Namely, Gly residues are present in the X-Gly-Gly-Gly-Y or X-Gly-Gly-Y sequence, as well as isolated in the Gly-rich sequences for *S.c.ricini* silk.[14] Here X and Y are the amino acids except for Gly residue. On the other hand, Gly residues are mainly present in the alternative sequences such as ...-Ala-Gly-Ala-Gly-Ala-Gly- in *B.mori* silk fibroin.

There is controversy about the conformation of the Gly residue in the Gly-rich sequence region of spider silk which is similar to the Gly-rich region of *S.c.ricini* silk fibroin.[30,32]

The Gly-rich region has been considered to be responsible for elasticity of spider silk.[32] Judging from the similar primary structure including Gly residues between *S.c.ricini* silk and spider silk, the sequences in spider silk seem to be mainly β-sheet. Actually, Thiel et al.[33] showed recently the presence of β-sheet structure including the Gly residue is required in order to interpret large crystal size predicted from careful X-ray diffraction analysis. Fukushima[36,37] prepared the seven repetitive polypeptides with a repeating sequence of the Gly-rich sequence of spider dragline silk by the recombinant DNA technique. The FT-IR data of the samples prepared as a cast film from formic acid showed β-sheet structure. Our conclusion is in agreement with these results.

Acknowledgment. T.A. acknowledges support from Bio-oriented Technology Research Advancement Institution.

References and Notes

(1) Asakura, T.; Kaplan, D. L. *Encyclopedia of Agricultural Science*; Arutzen, C. J., Ed.; Academic Press: New York, 1994; Vol. 4, pp 1−11.
(2) Hojo, N., Ed. *Zoku Kenshi no Kozo* (Structure of Silk Fibers); Shinshu University: Ueda, Japan, 1980.
(3) Mita, K.; Ichimura, S.; James, T. C. *J. Mol. Evol.* **1994**, *38*, 583.
(4) Marsh, R. E.; Corey, R. B.; Pauling, L. *Biochim. Biophys. Acta* **1955**, *16*, 1.
(5) Fraser, R. D. B.; MacRae, T. P. *Conformations of Fibrous Proteins and Related Synthetic Polypeptides*; Academic Press: New York, 1973.
(6) Takahashi, Y.; Gehoh, M.; Yuzuriha, K. *J. Polym. Sci., Polym. Phys. Ed.* **1991**, *29*, 889.
(7) Asakura, T.; Kuzuhara, A.; Tabeta, R.; Saito, H. *Macromolecules* **1985**, *18*, 1841.
(8) Saito, H.; Iwanaga, Y.; Tabeta, R.; Narita, M.; Asakura, T. *Chem. Lett.* **1983**, 427.
(9) Saito, H.; Tabeta, R.; Asakura, T.; Iwanaga, Y.; Shoji, A.; Ozaki, T.; Ando, I. *Macromolecules* **1984**, *17*, 1405.
(10) Saito, H.; Ishida, M.; Yokoi, M.; Asakura, T. *Macromolecules* **1990**, *23*, 83.
(11) Ishida, M.; Asakura, T.; Yokoi, M.; Saito, H. *Macromolecules* **1990**, *23*, 88.
(12) Asakura, T.; Demura, M.; Date, T.; Miyashita, M.; Ogawa, K.; Williamson, M. P. *Biopolymers* **1991**, *31*, 1529.
(13) Asakura, T.; Iwadate, M.; Demura, M.; Williamson, M. P. *Int. J. Biol. Macromol.* **1999**, *24*, 167.
(14) Personal communication.
(15) Yukuhiro, Y.; Kanda, T.; Tamura, T. *Insect Mol. Biol.* **1997**, *6*, 89.
(16) Asakura, T.; Murakami, T. *Macromolecules* **1985**, *18*, 2614.

(17) Asakura, T.; Kashiba, H.; Yoshimizu, H. *Macromolecules* **1988**, *21*, 644.
(18) Asakura, T.; Yoshimizu, H.; Yoshizawa, Y. *Macromolecules* **1988**, *21*, 2038.
(19) Iwadate, M.; Asakura, T.; Williamson, M. P. *J. Biomol. NMR* **1999**, *13*, 199.
(20) Nicholson, L. K.; Asakura, T.; Demura, M.; Cross, T. A. *Biopolymers* **1993**, *33*, 847.
(21) Cross, T. A. *Annu. Rep. NMR Spectrosc.* **1994**, *29*, 124.
(22) Demura, M.; Minami, M.; Asakura, T.; Cross, T. A. *J. Am. Chem. Soc.* **1998**, *120*, 1300.
(23) Asakura, T.; Sakaguchi, R.; Demura, M.; Ogawa, K.; Osanai, M. *Biotechnol. Bioeng.* **1993**, *41*, 245.
(24) Demura, M.; Yamazaki, Y.; Asakura, T.; Ogawa, K. *J. Mol. Struct.* **1998**, *441*, 155.
(25) Asakura, T.; Kawaguchi, Y.; Demura, M.; Osanai, M. *Insect Biochem.* **1988**, *18*, 531.
(26) Asakura, T.; Suzuki, H.; Tanaka, T. *J. Seric. Sci. Jpn.* **1985**, *54*, 504.
(27) Herzfeld, J.; Berger, A. E. *J. Chem. Phys.* **1980**, *73*, 6021.
(28) Teng, Q.; Cross, T. A. *J. Magn. Reson.* **1989**, *85*, 439.
(29) Asakura, T.; Yamazaki, Y.; Seng, K. W.; Demura, M. *J. Mol. Struct.* **1998**, *446*, 179.
(30) Simmons, A. H.; Michel, C. A.; Jelinski, L. W. *Science* **1996**, *271*, 84.
(31) Simmons, A.; Ray, E.; Jelinski, L. W. *Macromolecules* **1994**, *27*, 5235.
(32) Lewis, R. V. *Acc. Chem. Res.* **1992**, *25*, 392.
(33) Thiel, B. L.; Kunkel, D. D.; Viney, C. *Biopolymers* **1994**, *34*, 1089.
(34) Chou, P. Y.; Fasman, G. D. *Annu. Rev. Biochem.* **1978**, *47*, 251.
(35) Asakura, T.; Nakazawa, Y. Manuscript in preparation.
(36) Fukushima, Y. *Biopolymers* **1998**, *45*, 269.
(37) Fukushima, Y. *Chem. Lett.* **1998**, 939.

MA990442Z